

Exclusive Radiative B meson decays at Belle

Himansu Sahoo on behalf of the Belle Collaboration

Department of Physics and Astronomy, University of Hawaii, Honolulu, HI 96822, USA

himansu@phys.hawaii.edu

In this proceeding, we discuss recent results on exclusive radiative B meson decays from the Belle Collaboration. These decays are sensitive to right-handed currents from New Physics. In particular, we measure time-dependent CP violation parameters in $B^0 \rightarrow K_S^0 \pi^0 \gamma$ and $B^0 \rightarrow K_S^0 \rho^0 \gamma$ decays, using high-statistics data samples collected at the $\Upsilon(4S)$ resonance with the Belle detector at the KEKB asymmetric-energy e^+e^- collider. With the present statistics, these measurements are consistent with the standard model predictions. We also search for the radiative decay $B^0 \rightarrow \phi K^0 \gamma$ and report the first observation with a significance of 5.4σ , including systematic uncertainties.

1. Introduction

Rare radiative decays of B mesons play an important role in the search for physics beyond the standard model (SM) of electroweak interactions. These flavor changing neutral current decays are forbidden at tree level in the SM, but allowed through the electroweak penguin processes as in Fig. 1. Hence, they are sensitive to non-SM particles mediating the loop (for example, charged Higgs or SUSY particles), which could affect either the branching fraction or CP violation.

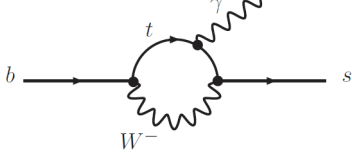


Figure 1: Feynman diagram for the radiative $b \rightarrow s\gamma$ decays, showing the SM loop process with the t -quark contribution.

In the SM, the photon emitted from a B^0 (\bar{B}^0) meson in the radiative $b \rightarrow s\gamma$ decays, is predominantly right-handed (left-handed). Therefore, the polarization of the photon carries information on the original b flavor and the time-dependent CP asymmetry is suppressed by the quark mass ratio ($2m_s/m_b$) [1]. In several models beyond the SM, the photon acquires an appreciable right-handed component due to the exchange of a virtual heavy fermion in the loop process, resulting in large values of mixing-induced CP asymmetries. The same argument holds in any multi-body final states $B^0 \rightarrow P^0 Q^0 \gamma$, where P^0 and Q^0 are charge-conjugate states [2] (e.g., $B^0 \rightarrow K_S^0 \rho^0 \gamma$, $B^0 \rightarrow \phi K_S^0 \gamma$) [3]. A non-zero value of CP asymmetry will be a clear hint of new physics.

2. Experimental Apparatus

The Belle detector is a large-solid-angle magnetic spectrometer that consists of a silicon vertex detector

(SVD), a 50-layer central drift chamber (CDC), an array of aerogel threshold Cherenkov counters (ACC), a barrel-like arrangement of time-of-flight scintillation counters (TOF), and an electromagnetic calorimeter (ECL) comprised of CsI(Tl) crystals located inside a superconducting solenoid coil that provides a 1.5 T magnetic field. An iron flux-return located outside the coil is instrumented to detect K_L^0 mesons and to identify muons (KLM). The detector is described in detail elsewhere [4]. Two different inner detector configurations were used. For the first sample of 152×10^6 $B\bar{B}$ pairs, a 2.0 cm radius beampipe and a 3-layer silicon vertex detector (SVD1) were used; for the latter samples, a 1.5 cm radius beampipe, a 4-layer silicon detector (SVD2), and a small-cell inner drift chamber were used.

3. Analysis Technique

At the KEKB asymmetric-energy e^+e^- (3.5 on 8.0 GeV) collider [5], the $\Upsilon(4S)$ is produced with a Lorentz boost of $\beta\gamma = 0.425$ nearly along the z axis, which is defined as opposite to the e^+ beam direction. In the decay chain $\Upsilon(4S) \rightarrow B^0 \bar{B}^0 \rightarrow f_{\text{rec}} f_{\text{tag}}$, where one of the B mesons decays at time t_{rec} to a final state f_{rec} , which is our signal mode, and the other decays at time t_{tag} to a final state f_{tag} that distinguishes between B^0 and \bar{B}^0 , the decay rate has a time dependence given by

$$\mathcal{P}(\Delta t) = \frac{e^{-|\Delta t|/\tau_{B^0}}}{4\tau_{B^0}} \left\{ 1 + q \cdot \left[\mathcal{S} \sin(\Delta m_d \Delta t) + \mathcal{A} \cos(\Delta m_d \Delta t) \right] \right\}. \quad (1)$$

Here \mathcal{S} and \mathcal{A} are the CP -violation parameters, τ_{B^0} is the neutral B lifetime, Δm_d is the mass difference between the two neutral B mass eigenstates, $\Delta t = t_{\text{rec}} - t_{\text{tag}}$, and the b -flavor charge q equals $+1$ (-1) when the tagging B meson is identified as B^0 (\bar{B}^0). Since the B^0 and \bar{B}^0 are approximately at rest in the $\Upsilon(4S)$ center-of-mass system (cms), Δt can be

determined from the displacement in z between the f_{rec} and f_{tag} decay vertices: $\Delta t \simeq \Delta z/(\beta\gamma c)$, where c is the speed of light.

3.1. Flavor Tagging and Vertex Reconstruction

The b flavor of the accompanying B meson is identified by a tagging algorithm [6] that categorizes charged leptons, kaons, and Λ baryons found in the event. The algorithm returns two parameters: the b -flavor charge q , and r , which measures the tag quality and varies from $r = 0$ for no flavor discrimination to $r = 1$ for unambiguous flavor assignment. If $r < 0.1$, the accompanying B meson provides negligible tagging information and we set the wrong tag probability to 0.5. Events with $r > 0.1$ are divided into six r intervals. The wrong tag fractions for the six r intervals, w_l ($l = 1, 6$) and possible differences in w_l between B^0 and \bar{B}^0 decays (Δw_l) are determined using high-statistics control samples of semi-leptonic and hadronic $b \rightarrow c$ decays [7, 8].

The vertex position of the signal-side decay is reconstructed from the K_S^0 trajectory in $B^0 \rightarrow K_S^0 \pi^0 \gamma$ and from the daughters of the ρ^0 in $B^0 \rightarrow K_S^0 \rho^0 \gamma$ mode, with a constraint on the interaction point. The tracks are required to have enough hits in the SVD for vertexing. The tag-side B vertex is determined from well reconstructed tracks that are not assigned to the signal side.

We determine \mathcal{S} and \mathcal{A} by performing an unbinned maximum-likelihood (UML) fit to the observed Δt distribution. The likelihood function is

$$\mathcal{L}(\mathcal{S}, \mathcal{A}) = \prod_i \mathcal{P}_i(\mathcal{S}, \mathcal{A}; \Delta t_i), \quad (2)$$

where the product includes all events in the fit. The probability density function (PDF) is given by

$$\mathcal{P}_i = (1 - f_{\text{ol}}) \int \left[\sum_j f_j \mathcal{P}_j(\Delta t') R_j(\Delta t_i - \Delta t') \right] d(\Delta t') + f_{\text{ol}} P_{\text{ol}}(\Delta t_i). \quad (3)$$

where j runs over the signal and all background components. The fractions of each component (f_j) depend on the r region and are calculated on an event-by-event basis as a function of the fitted variable. R_j is the Δt resolution function and $P_{\text{ol}}(\Delta t)$ is a broad Gaussian function that represents an outlier component with a small fraction f_{ol} . The only free parameters in the final fit are \mathcal{S} and \mathcal{A} , which are determined by maximizing the likelihood function given by Eq. 2. We define the raw asymmetry in each Δt bin by $(N_+ - N_-)/(N_+ + N_-)$, where N_+ (N_-) is the number of observed candidates with $q = +1$ (-1).

4. Time-dependent Analysis of $B^0 \rightarrow K_S^0 \pi^0 \gamma$

This analysis is done in Belle using 535×10^6 $B\bar{B}$ pairs [9]. Since the time-dependent CP asymmetry is not expected to change significantly as a function of $K_S \pi^0$ invariant mass, we perform two measurements: one for $B^0 \rightarrow K^{*0}(\rightarrow K_S^0 \pi^0) \gamma$ by requiring $M_{K_S^0 \pi^0}$ to lie in the range $0.8 < M_{K_S^0 \pi^0} < 1.0$ GeV/c^2 , and the other for the full range of $M_{K_S^0 \pi^0}$ below 1.8 GeV/c^2 .

The primary signature of these type of decays is the high energy prompt photon. They are selected from isolated ECL clusters, with center-of-mass (cms) energy in the range 1.4 to 3.4 GeV . The polar angle of the photon direction in the laboratory frame is restricted to the barrel region of the ECL ($33^\circ < \theta_\gamma < 128^\circ$) for SVD1 data, but is extended to the end-cap regions ($17^\circ < \theta_\gamma < 150^\circ$) for SVD2 data due to the reduced material in front of the ECL. The selected photon candidates are required to be consistent with isolated electromagnetic showers, i.e., 95% of the energy in an array of 5×5 CsI(Tl) crystals should be concentrated in an array of 3×3 crystals and should have no charged tracks associated with it. We also remove photons from $\pi^0(\eta) \rightarrow \gamma\gamma$ using a likelihood function described in Ref. [10]. Neutral kaons (K_S^0) are reconstructed from two oppositely charged pions that have an invariant mass within ± 6 MeV/c^2 of the K_S^0 mass. Neutral pions (π^0) are formed from two photons with an invariant mass within ± 16 MeV/c^2 of the π^0 mass.

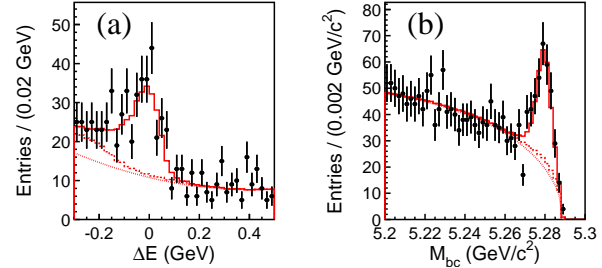


Figure 2: (a) ΔE distribution within the M_{bc} signal slice and (b) M_{bc} distribution within the ΔE signal slice for the whole $M_{K_S^0 \pi^0}$ region. Points with error bars are data. The solid curves show the fit results. The dotted curves show the $q\bar{q}$ background contributions, while the dashed curves show the sum of $q\bar{q}$ and $B\bar{B}$ background contributions.

The B candidates are identified using two kinematic variables: the energy difference $\Delta E \equiv E_B^{\text{cms}} - E_{\text{beam}}^{\text{cms}}$ and the beam-energy-constrained mass $M_{bc} \equiv \sqrt{(E_{\text{beam}}^{\text{cms}})^2 - (p_B^{\text{cms}})^2}$, where $E_{\text{beam}}^{\text{cms}}$ is the beam energy in the cms, and E_B^{cms} and p_B^{cms} are the cms energy and momentum, respectively, of the reconstructed B candidate. The signal region in ΔE and M_{bc} , which

is used for the measurements of CP -violating parameters, is defined as $-0.2 \text{ GeV} < \Delta E < 0.1 \text{ GeV}$ and $5.27 \text{ GeV}/c^2 < M_{bc} < 5.29 \text{ GeV}/c^2$.

After all selections are applied, we obtain 4078 candidates in the ΔE - M_{bc} fit region, of which 406 are in the signal box. The signal yield is obtained from an UML fit to the ΔE - M_{bc} distribution as shown in Fig. 2. Figure 3 shows the Δt distributions of the events with $0.5 < r \leq 1.0$ for $q = +1$ and $q = -1$ and the raw asymmetry. The CP violation parameters for $K_S^0 \pi^0 \gamma$ for the full $K_S^0 \pi^0$ invariant mass region as well as for the mass region around $K^*(892)^0$ are summarized in Table I.

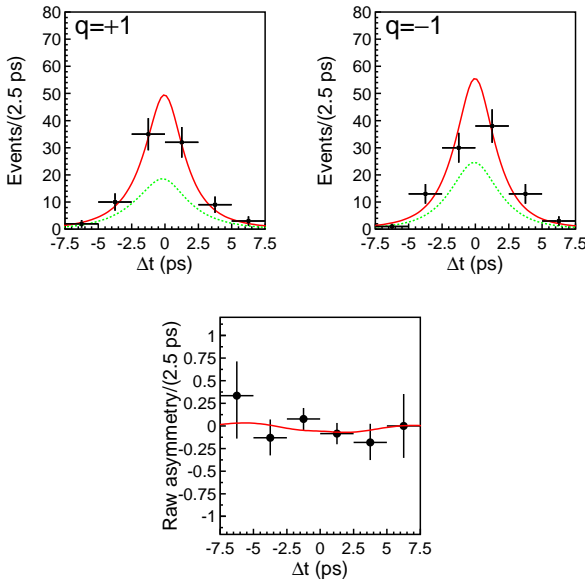


Figure 3: (Top) Proper time distributions for $B^0 \rightarrow K_S^0 \pi^0 \gamma$ for $q = +1$ (left) and $q = -1$ (right) with $0.5 < r \leq 1.0$. The solid curve shows the total and dashed curve shows the signal component. (Bottom) Asymmetry in each Δt bin with $0.5 < r \leq 1.0$. The solid curve shows the result of the UML fit.

5. Time-dependent Analysis of $B^0 \rightarrow K_S^0 \rho^0 \gamma$

The first measurement of time-dependent CP asymmetry in $B^0 \rightarrow K_S^0 \rho^0 \gamma$ mode was performed by Belle using $657 \times 10^6 B\bar{B}$ pairs [11]. The advantage of this mode is that the B^0 decay vertex can be reconstructed from two charged pions from the ρ^0 decays, thus avoiding the complications and efficiency loss from K_S^0 vertexing. The expected \mathcal{S} has opposite sign to that of $B^0 \rightarrow K_S^0 \pi^0 \gamma$.

The signal is reconstructed in the decay $B^0 \rightarrow K_S^0 \rho^0 \gamma$ with $\rho^0 \rightarrow \pi^+ \pi^-$ and $K_S^0 \rightarrow \pi^+ \pi^-$. The selection criteria for high energy prompt photon and neu-

tral kaons are same as those described in section 4, except the photons are required to lie in the barrel region of the ECL and the K_S^0 invariant mass should be within $\pm 15 \text{ MeV}/c^2$ of its nominal mass. We also reconstruct the $B^+ \rightarrow K^+ \pi^- \pi^+ \gamma$ decay to study the $K\pi\pi$ system and to serve as a control sample. The $K^+ \pi^- \pi^+$ and $K_S^0 \pi^+ \pi^-$ invariant masses are required to be less than $1.8 \text{ GeV}/c^2$. The B candidates are selected from the $K_S^0 \pi^+ \pi^- \gamma$ sample by requiring the $\pi^+ \pi^-$ invariant mass to lie in the ρ^0 region, $0.6 \text{ GeV}/c^2 < m_{\pi\pi} < 0.9 \text{ GeV}/c^2$. Since the ρ^0 is wide, other modes that are not self-conjugate, such as $K^{*+} \pi^- \gamma$ may also contribute. Therefore, we first measure the effective CP -violating parameters, \mathcal{S}_{eff} and \mathcal{A}_{eff} , using the final sample and then convert them to the CP -violating parameters of $B^0 \rightarrow K_S^0 \rho^0 \gamma$ using a dilution factor \mathcal{D} , described in Ref. [11].

The signal is extracted from an UML fit to the M_{bc} distribution as shown in Fig. 4. The requirement $-0.1 \text{ GeV} < \Delta E < 0.08 \text{ GeV}$ is applied. We obtain 299 events in the signal M_{bc} region after vertexing. Out of these we find a signal of 212 ± 17 events with a fraction of 6.0% self-cross-feed (SCF), 53.4 ± 2.6 continuum, along with 7.8 $K^* \gamma$, 21.5 other $X_s \gamma$, and 9.0 $B\bar{B}$ events.

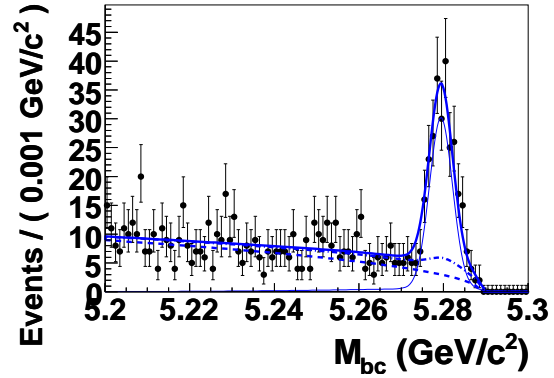


Figure 4: M_{bc} distributions for $B^0 \rightarrow K_S^0 \pi^+ \pi^- \gamma$ events. Points with error bars are data. The curves show the results from the r dependent M_{bc} fit. The dashed and dash-dotted curves are the $q\bar{q}$ and all background. The thin curve is the total signal including SCF and the thick curve is the total PDF.

We obtain $\mathcal{S}_{\text{eff}} = 0.09 \pm 0.27(\text{stat.})^{+0.04}_{-0.07}(\text{syst.})$ and $\mathcal{A}_{\text{eff}} = 0.05 \pm 0.18(\text{stat.}) \pm 0.06(\text{syst.})$ from an UML fit to the observed Δt distribution. The parameter \mathcal{S}_{eff} is related to \mathcal{S} for $K_S^0 \rho^0 \gamma$ with a dilution factor $\mathcal{D} \equiv \mathcal{S}_{\text{eff}}/\mathcal{S}_{K_S^0 \rho^0 \gamma}$, that depends on the $K^{*\pm} \pi^\mp$ components and allows for interference:

$$\mathcal{D} = \frac{\int [|F_A|^2 + 2 \text{Re}(F_A^* F_B) + F_B^*(\bar{K}) F_B(K)]}{\int [|F_A|^2 + 2 \text{Re}(F_A^* F_B) + |F_B|^2]}, \quad (4)$$

where F_A, F_B are photon-helicity averaged amplitudes for $B^0 \rightarrow K_S^0 \rho^0 (\pi^+ \pi^-) \gamma$ and $B^0 \rightarrow K^{*\pm} (K_S^0 \pi^\pm) \pi^\mp \gamma$,

respectively. The factors $F_B(\bar{K})$, $F_B(K)$ distinguish between $K^{*-}\pi^+\gamma$ and $K^{*+}\pi^-\gamma$. The phase space integral is over the ρ^0 region. We measure the dilution factor \mathcal{D} to be $0.83^{+0.19}_{-0.03}$ from the charged mode $B^+ \rightarrow K^+\pi^-\pi^+\gamma$ using a combination of various kaonic resonances with spin ≥ 1 to model the $K\pi\pi$ system. By combining it with \mathcal{S}_{eff} , we obtain $\mathcal{S}_{K_S\rho^0\gamma} = 0.11 \pm 0.33(\text{stat.})^{+0.05}_{-0.09}(\text{syst.})$. The fits to the observed Δt distributions and the raw asymmetry are shown in the Fig. 5. The fit results are summarized in Table I. Figure 6 shows the distributions for the $m_{\pi\pi}$ spectrum.

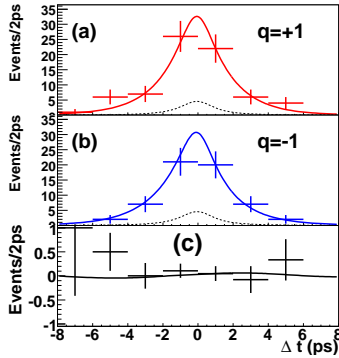


Figure 5: Fit projections on the Δt distributions with (a) $q = +1$ and (b) $q = -1$ for events with $r > 0.5$. The solid curves are the fit while the dashed curves show the background contributions. The raw asymmetry as a function of Δt is shown in (c) with a fit curve superimposed.

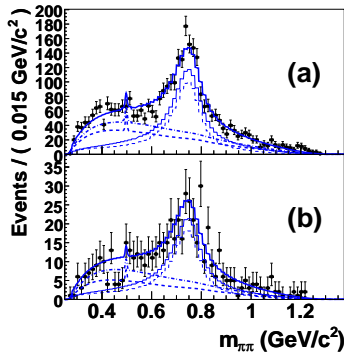


Figure 6: $m_{\pi\pi}$ distributions for (a) $B^+ \rightarrow K^+\pi^-\pi^+\gamma$ and (b) $B^0 \rightarrow K_S^0\pi^+\pi^-\gamma$. The curves follow the convention in Fig. 4. The thin dashed curve is the correctly reconstructed $B \rightarrow K_1(1270)\gamma$ signal.

6. First Observation of $B^0 \rightarrow \phi K_S^0 \gamma$ decay

This decay mode has advantages similar to $B^0 \rightarrow K_S^0 \rho^0 \gamma$ in the search for new physics. Here the B^0 decay vertex can be reconstructed from the two charged

Table I Results of the fits to the Δt distributions. The first errors are statistical and the second errors are systematic.

Decay Mode	\mathcal{S}	\mathcal{A}
$B^0 \rightarrow K^*(892)^0 \gamma$	$-0.32^{+0.36}_{-0.33} \pm 0.05$	$-0.20 \pm 0.24 \pm 0.05$
$B^0 \rightarrow K_S \pi^0 \gamma$	$-0.10 \pm 0.31 \pm 0.07$	$-0.20 \pm 0.20 \pm 0.06$
$B^0 \rightarrow K_S \rho^0 \gamma$	$0.11 \pm 0.33^{+0.05}_{-0.09}$	$0.05 \pm 0.18 \pm 0.06$

kaons from the ϕ decay. The branching fractions for the charged $\phi K \gamma$ mode and an upper limit on the neutral mode have already been reported by the Belle [12] using $96 \times 10^6 B\bar{B}$ pairs. We search for the neutral mode using the full data sample, nearly eight times larger than was used in our previous measurement and report the first observation with a significance of 5.4σ .

The signal is reconstructed in the decay $B^+ \rightarrow \phi K^+ \gamma$ and $B^0 \rightarrow \phi K_S^0 \gamma$, with $\phi \rightarrow K^+ K^-$ and $K_S^0 \rightarrow \pi^+ \pi^-$. The invariant mass of the ϕ candidates is required to be within $-0.01 < M_{K^+ K^-} - m_\phi < +0.01$ GeV/c², where m_ϕ denotes the world-average ϕ mass [13]. The selection criteria for the high energy prompt photon and neutral kaons are the same as those described in section 4, except the photons are required to lie in the barrel region and the invariant mass of the $\pi^+ \pi^-$ combinations has to be in the range 0.482 GeV/c² $< M_{\pi^+ \pi^-} < 0.514$ GeV/c². The B candidates are selected with a requirement 5.2 GeV/c² $< M_{bc} < 5.3$ GeV/c² and -0.3 GeV $< \Delta E < 0.3$ GeV. We define the signal region as 5.27 GeV/c² $< M_{bc} < 5.29$ GeV/c² and -0.08 GeV $< \Delta E < 0.05$ GeV.

The dominant background is from the continuum process, which is suppressed by a requirement on likelihood ratio from event shape variables and the B flight direction. In the $B^0 \rightarrow \phi K_S^0 \gamma$ mode, some backgrounds from $b \rightarrow c$ decays, like $D^0 \pi^0$, $D^0 \eta$ and $D^- \rho^+$ peak in the M_{bc} distribution. We remove these backgrounds by applying a veto on the ϕK_S^0 invariant mass. The non-resonant background $B \rightarrow K^+ K^- K \gamma$, which peaks in the ΔE - M_{bc} signal region, is estimated using the ϕ mass sideband in data.

The signal yield is obtained from an extended UML fit to the two-dimensional ΔE - M_{bc} distribution. The projections of the fit results into ΔE and M_{bc} are shown in Fig. 7 and the fit results are summarized in Table II. The fit yields a signal of $(136 \pm 17) B^+ \rightarrow \phi K^+ \gamma$ and $(35 \pm 8) B^0 \rightarrow \phi K_S^0 \gamma$ candidates. The signal in the charged mode has a significance of 9.6σ , whereas that for the neutral mode is 5.4σ , including systematic uncertainties.

We also search for a possible contribution from kaonic resonances decaying to ϕK . To unfold the $M_{\phi K}$ distribution, we subtract all possible backgrounds and correct the ϕK invariant mass for the efficiency. The background-subtracted and efficiency-corrected $M_{\phi K}$ distributions are shown in Fig. 8.

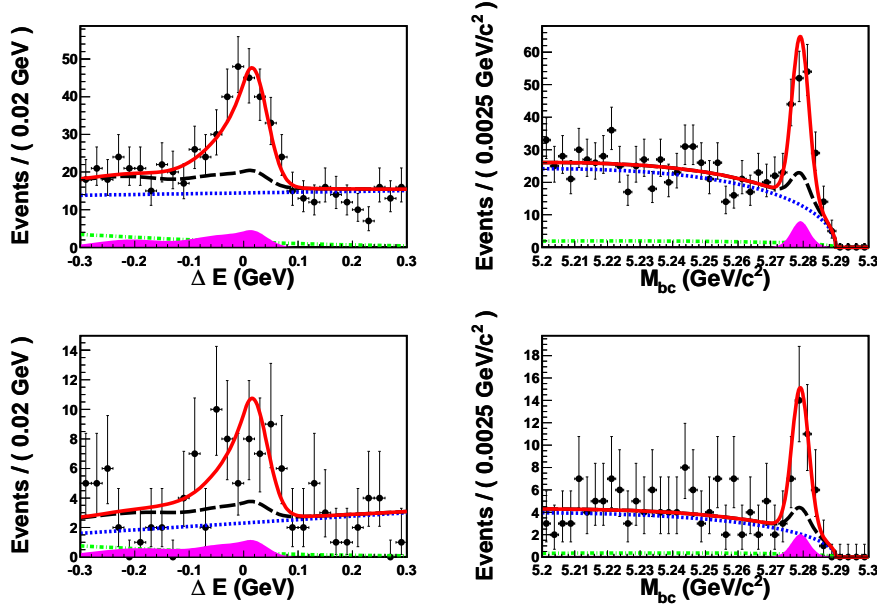


Figure 7: The ΔE and M_{bc} projections for $B^+ \rightarrow \phi K^+ \gamma$ (upper) and $B^0 \rightarrow \phi K_S^0 \gamma$ (lower). The points with error bars represent the data. The different curves show the total fit function (solid, red), total background function (long-dashed, black), continuum component (dotted, blue), the $b \rightarrow c$ component (dashed-dotted, green) the non-resonant component as well as other charmless backgrounds (filled histogram, magenta).

Table II The signal yields (Y), corrected efficiencies (ϵ), branching fractions (\mathcal{B}) and significances (S) for the $B^+ \rightarrow \phi K^+ \gamma$ and $B^0 \rightarrow \phi K^0 \gamma$ decay modes.

Mode	Y	ϵ (%)	\mathcal{B} (10^{-6})	S (σ)
$\phi K^+ \gamma$	136 ± 17	15.3 ± 0.1	$2.34 \pm 0.29 \pm 0.23$	9.6
$\phi K^0 \gamma$	35 ± 8	10.0 ± 0.1	$2.66 \pm 0.60 \pm 0.32$	5.4

Nearly 72% of the signal events are concentrated in the low-mass region ($1.5 < M_{\phi K} < 2.0$ GeV/c^2). It is clear that the observed ϕK mass spectrum differs significantly from that expected in a three-body phase-space decay.

7. Summary

In summary, we report the first observation of radiative $B^0 \rightarrow \phi K_S^0 \gamma$ decays in Belle using a data sample of 772×10^6 $B\bar{B}$ pairs. The observed signal yield is (35 ± 8) with a significance of 5.4σ including systematic uncertainties. We also precisely measure the $B^+ \rightarrow \phi K^+ \gamma$ branching fraction with a significance of 9.6σ . The signal events are mostly concentrated at low ϕK mass, which is similar to a two-body radiative decay. We report the measurements of time-dependent CP violation parameters in $B^0 \rightarrow K_S^0 \pi^0 \gamma$ and $B^0 \rightarrow K_S^0 \rho^0 \gamma$ decays, using 535×10^6 and 657×10^6 $B\bar{B}$ pairs, respectively. The Heavy Flavor Averaging Group (HFAG) [14] summary of the measurements of

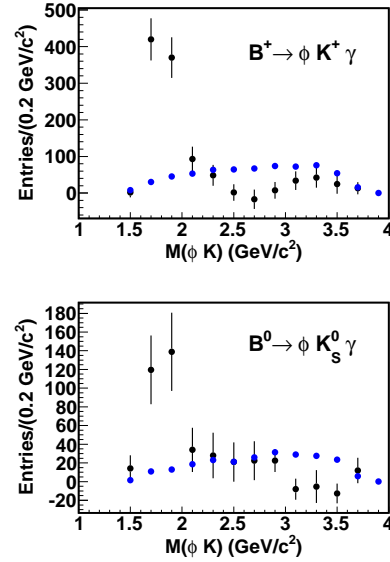


Figure 8: The background-subtracted and efficiency-corrected ϕK mass distributions for $B^+ \rightarrow \phi K^+ \gamma$ (upper) and $B^0 \rightarrow \phi K_S^0 \gamma$ (lower). The points with error bars represent the data. The yield in each bin is obtained by the fitting procedure described in the text. The three-body phase-space model from the MC simulation is shown by the circles (blue).

the parameter S in $b \rightarrow s\gamma$ modes by the Belle and BaBar is shown in Figure 9. With the present statistics, these measurements are consistent with the stan-

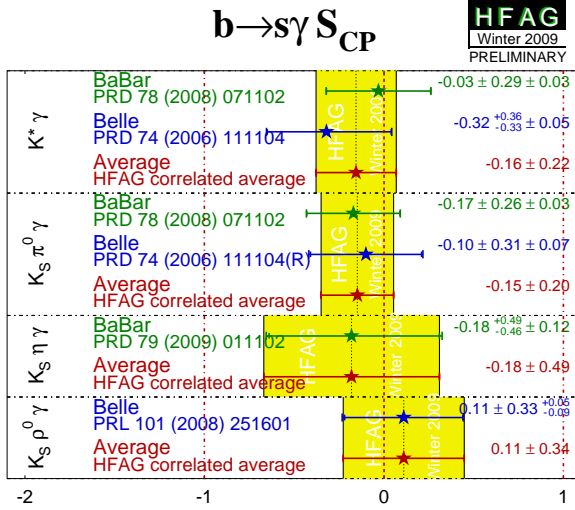


Figure 9: Summary of Belle and BaBar measurements of $b \rightarrow s \gamma S_{CP}$.

dard model predictions and there is no indication of New Physics from right-handed currents in radiative B decays. The neutral $B^0 \rightarrow \phi K_S^0 \gamma$ mode has enough statistics for a future measurement of time-dependent CP violation. More luminosity is necessary for a precise test of the SM.

Acknowledgments

We thank the KEKB group for excellent operation of the accelerator, the KEK cryogenics group for efficient solenoid operations, and the KEK computer group and the NII for valuable computing and SINET3 network support. We acknowledge support from MEXT, JSPS and Nagoya's TLP RC (Japan); ARC and DIISR (Australia); NSFC (China); DST

(India); MEST, KOSEF, KRF (Korea); MNiSW (Poland); MES and RFAAE (Russia); ARRS (Slovenia); SNSF (Switzerland); NSC and MOE (Taiwan); and DOE (USA).

References

- [1] D. Atwood, M. Gronau and A. Soni, Phys. Rev. Lett. **79**, 185 (1997).
- [2] D. Atwood, T. Gershon, M. Hazumi and A. Soni, Phys. Rev. D **71**, 076003 (2005).
- [3] Throughout this paper, the inclusion of the charge-conjugate decay mode is implied unless otherwise stated.
- [4] A. Abashian *et al.* (Belle Collaboration), Nucl. Instrum. Methods Phys. Res., Sect. A **479**, 117 (2002).
- [5] S. Kurokawa and E. Kikutani, Nucl. Instrum. Methods Phys. Res., Sect. A **499**, 1 (2003), and other papers included in this volume.
- [6] H. Kakuno *et al.*, Nucl. Instrum. Methods Phys. Res., Sect. A **533**, 516 (2004).
- [7] K. Abe *et al.* (Belle Collaboration), Phys. Rev. D **71**, 072003 (2005).
- [8] K-F. Chen *et al.* (Belle Collaboration), Phys. Rev. D **72**, 012004 (2005).
- [9] Y. Ushiroda *et al.* (Belle Collaboration), Phys. Rev. D **74**, 111104(R) (2006).
- [10] P. Koppenburg *et al.* (Belle Collaboration), Phys. Rev. Lett. **93**, 061803 (2004).
- [11] J. Li *et al.* (Belle Collaboration), Phys. Rev. Lett. **101**, 251601 (2008).
- [12] A. Drutskoy *et al.* (Belle Collaboration), Phys. Rev. Lett. **92**, 051801 (2004).
- [13] C. Amsler, *et al.*, Physics Letters **B 667**, 1 (2008).
- [14] Heavy Flavor Averaging Group, winter 2009 update. Check their webpage for updated results: <http://www.slac.stanford.edu/xorg/hfag/>.